Long-distance Localization of 4Cr13 Stainless Ball-pocket in Radiative Region

he huayan (hehy@ihep.ac.cn)
Institute of High Energy Physics
wang guangyuan
Institute of High Energy Physics

Original Article

Keywords: Radiation, 4Cr13, Ball- pocket, Locating structure, Comprehensive mechanical properties, Machining error

Posted Date: December 20th, 2021

DOI: https://doi.org/10.21203/rs.3.rs-1112484/v1

Abstract

Radiation caused by high-energy particles would speed up the damage of accelerator equipment. The high residual radiation from equipment affects staff health as well. Intelligent robots receive various limits to replace human in completing complex and time-consuming maintenance in radiative region because of high sensitivity to radiation. The 4Cr13 stainless ball-pocket was designed in the study of localization in long distance with the advantages of the conical fit technology. Moreover, the 4Cr13 stainless ball-pocket and bearing ball combine and form a locating structure, which has good performance on automatic aligning, self-locking and rapid dismantling. The comprehensive mechanical properties of 4Cr13 stainless ball-pocket were studied and optimized based on three heat treatment methods of martensite steel containing chromium alloy. The study of machining conditions states that compared with the design accuracy of localization, the machining error retains definite allowance. The 4Cr13 stainless ball-pocket successfully exhibits sufficient supporting strength, wearing reducing and radiation resistance. This study shows that 4Cr13 stainless ball-pocket has better fitting precision than 0.2 mm in practice. This study could offer a reliable strategy and measure for long-distance localization in other dangerous regions.

1. Introduction

China Spallation Neutron Source is a national scientific project. It contains a series of proton or neutron transporting equipment. Equipment service life considerably decreases because of radiation caused by high-energy particles. The maximum residual radiation dose rate to staff is 10 Sv per hour [1]. Maintaining or resetting such equipment through the conventional method at short distance is clearly not feasible. With the development of autoimmunization technique, intelligent assist devices have been put into use for installation in danger region, such as special robot system, manipulator, machine vision and control system. However, the service life of these electronic equipment decreases after high-dose radiation. Therefore, it is hard to carry out complex and long operations. The ionization and dissociation of airs around the equipment generates ozone ions, accelerating equipment aging. Thus, it is not the norm to reserve additional space for automatic operation at short distances. At present, intelligent robots always receive various limits to replace manpower in radiative regions. Therefore, discussion on other viable and reliable solution of equipment localization in long distance is valuable.

The equipment layout of proton transporting line nearby the beam target is shown in figure 1. The accelerator equipment was divided into seven units. Each unit includes two sections: the accelerator equipment for long-distance hoisting and the ground support, as shown in figure 2 [2]. In this study, the 4Cr13 stainless ball-pocket was designed and combined with bearing ball in this study [3]. The 4Cr13 stainless ball-pockets were equipped into two sections of each unit. When the accelerator equipment was hoisted at long distance, the bearing ball was driven to roll slowly on the conical surfaces of the ball-pocket until the axes were all in mutual coincidence. With the bearing ball as the guide, the equipment was installed to the design location and then easily dismantled, providing the basis of long-distance localization in radiative region.

The 4Cr13 stainless ball-pockets should overcome the interference of force deformation, wearing and radiation aging to realize the design accuracy of long-distance localization [4]. Accordingly, the study on long-distance localization of 4Cr13 stainless ball-pocket was carried out in four parts: structural design, material selection, strength analysis, and form machining.

2. Structural Design

The equipment localization process of the 4Cr13 stainless ball-pocket consists of two steps: pre-alignment and automatic alignment of long distance. The flowchart of localization is shown in figure 3. The components of the two sections are pre-aligned based on their relative coordinates by using a laser tracker [5]. While the ground support ultimately is fixed on the accelerator tunnel, the mechanical-guided accelerator equipment could automatically fit the ground support from coarse to fine in long distance. The self-weight of the equipment would voluntarily restrict degree of freedom on the elevation direction, while multiple mechanical fits of ball-pockets restrict other 5 DOFs, eventually putting all targets in the right place. On the contrary, removing the load of self-weight can realize rapid dismantling.

The locating structure of 4Cr13 stainless ball-pockets is shown in figure 4. It is an optimized conical structure, whereas the ball-pocket is regarded as the outer conical surface. The locating structure consists of two 4Cr13 stainless ball-pockets, a bearing ball with diameter of 70 mm, a retainer ring, and two base sheets. The 4Cr13 stainless ball-pocket is assembled to the support through the base sheet. The minimum clearance between the retainer ring and the bearing ball is 0.8 mm, ensuring the rolling motion of ball-pocket during the automatic alignment, decreasing material wear loss. In general, the accelerator equipment realizes high precision and self-locking through peculiar locating structure of 4Cr13 stainless ball-pocket.

3. Material Selection

In this study, material of the ball-pocket should have excellent performance in resisting of radiation, impact, and wear [6]. It is supposed to have enough stiffness and strength to decrease the deformation and wear behaviors. For accelerator equipment with overall weight of 15t, any of non-metallic or organic polymer material cannot provide both sufficient mechanical strength and radioresistance. Therefore, the conventional and easily accessible steel is chosen to manufacture the ball-pocket ultimately.

The structure of the body-centered cubic lattice with an alloy element, such as alloy Cr□W□αFe alloy, has high hardness. According to appropriate parameters setting of heat treatment processes, such as quenching or normalizing temperature, lower bainite and martensite could have excellent properties of high stiffness and toughness [7]. Moreover, material of 4Cr13 stainless is a kind of martensite steel. Its element composition is summarized in table 1. The existence of chromium element promotes high strength, toughness, hardenability and excellent tempering stability [8]. The hardness of quenched 4Cr13 steel could be higher than 50HRC. Then the average tensile strength of 4Cr13 stainless steel could be greater than 1700MPa. Given its excellent comprehensive mechanism properties, 4Cr13 was chosen for

the ball-pocket. The material of retainer ring is any steel that is not easy rusty. The material of base sheet can be conventional carbon steel with enough support strength. In conclusion, the materials of the locating structure of figure 4 are summarized in table 2.

Table 1 Element compositions of 4Cr13 (mass content %)

C	Si	Mn	S	P	Cr	Ni
0.4	≤0.6	≤0.8	≤0.03	≤0.035	13	≤0.6

Table 2 Materials of the locating structure

elements	Material	Density	Elastic modulus	Poisson's radio
Ball-pocket	4Cr13	7750 kg/m^3	206 GPa	0.25
Base sheet	Q235	7850 kg/m^3	210 GPa	0.27
Retainer ring	304	7930 kg/m^3	190 GPa	0.25
Bearing ball	GCr15	7810 kg/m^3	208 GPa	0.3

4. Strength Analysis

Suppose that machine errors of all components are equal. In this case, the inner conical surface of the bearing ball squarely contacts the outer conical surface of the 4Cr13 stainless ball-pocket. After the alignment of long-distance hoisting is completed, the force load of 4Cr13 stainless ball-pocket comes from the total self-weight (15 tons). However, the alignment in long distance is based on the use of overhead traveling crane. Then, the acceleration in the elevation direction is inevitable. In practice, the amplifying coefficient of force load is 1.5. Considering the total supporting weight of the four ball-pockets (15 tons), we could calculate that each pressure load is equal to 56.25KN.

The stress distribution of the locating structure was simulated using finite element software. The results are shown in figure 5. Figure 5(a) shows that the maximum equivalent stress of the locating structure is 104.1MPa, which is undertaken by the bearing ball. Figure 5(b) shows that the maximum deformation is 0.02 mm. Figure 5(c) shows the stress distribution of the ball-pocket, and the maximum equivalent stress of the ball-pocket is 57.4MPa.

For component used in danger region, the empirical value of the high strength yield is 0.6 [9]. The simulated results indicate that the ball-pocket is supposed to have a strength higher than 95.4MPa. The finding offers further support for the material selection and provides a standard reference for the following heat treatment.

5. Form Machining

The process of form machining is mainly focused on heat treatment and conical forming technology. The first part obtains the sufficient mechanical properties of 4Cr13 stainless steel, and the other one forms the most important conical shape for automatic alignment. The mechanical properties play a leading role in the processing method.

5.1 Heat treatment

Strength and toughness are important mechanical properties of the 4Cr13 stainless ball-pocket. These properties exhibit surface resistance to plastic deformation, wear, and destructive capability. Tensile strength can convert mutually into hardness. Hardness testing has many good advantages, such as quick, simple and no sample destruction [10]. We can detect whether the tensile strength is safe and reliable by measuring hardness values. The conversion between tensile strength and Vickers hardness according to DIN50150 standard is shown in table 3.

Table 3 Conversion between tensile strength and Vickers hardness.

Vickers hardness	640	600	550	520	510	500	490
Tensile strength	2145	1995	1810	1700	1665	1630	1595

The key parameters of heat treatment mainly include quenching temperature, quenching medium and temper cooling to obtain homogeneous and fine martensite organization [11]. If the quenching temperature is too high, coarse martensite negatively affects toughness, probably leading to cracks under the impact. Conversely, the lower temperature may increase ferrite content and hardness reduction [12]. The cooling speed should be supposed to be fast enough, but simultaneously it would not lead to excessive internal stress and crack formation. There are three different processes of heat treatment were studied to obtain excellent microstructure: empirical process a, optimized process b and c with cryogenic treatment and tempering, as shown in figure 6. The hardness of cross-sectional points was measured in increasing depth. The results of the ball-pocket optimized under the three processes are shown in figure 7.

Figure 7 shows that the maximum hardness of ball-pocket by empirical process a is 706HV, the minimum is 597HV, and the relative difference value is 109HV. The results indicate that the microstructure by empirical process a is relatively rough and uneven, with large residual internal stress probably [13]. The structure has a negative effect on impact toughness, possibly leading to different deformation of the four ball- pockets during automatic alignment. The scenario is harmful to localization precision.

We lowered quenching temperature and added measurement of cryogenic treatment as well as tempering treatment based on the process a to obtain refined martensite, as shown in figure 6(b). The measuring results of hardness shown in figure 7 indicate that the maximum hardness of ball-pocket is 548HV, the minimum is 519HV, and the relative difference value is 29HV. Thus, uniform martensite was obtained after improvement, but the overall hardness was apparently low. Process b of heat treatment realized martensite refinement. Modifying the parameters further is still necessary to improve the hardness values [14].

The third process of heat treatment is shown in figure 6(c). The quenching temperature, cooling medium, and cooling method were optimized further. As shown in figure 7, the maximum hardness of ball-pocket is 644HV, the minimum is 596HV, and the difference between them is 48HV. The cross-sectional image of the internal microstructure of the 4Cr13 stainless ball-pocket is shown in figure 8. In particular, the measures of mineral oil at 200Pa and cryogenic treatment have a positive effect on improving hardness without producing cracks in rapid cooling. In addition, the tempering treatment promoted the conversion of the retained austenite, thereby increasing hardness and wearability. The grain refining effect on martensite could be further studied by increasing tempering time or lowering quenching temperature if necessary. In summary, the 4Cr13 stainless ball-pocket by process c has a relatively fine and uniform structure and tensile strength is higher than 1995MPa, which successfully meets the mechanical strength requirement for localization.

In practice, cracks tend to occur during quenching and rapid cooling in practice. As shown in figure 9, the 4Cr13 stainless ball-pocket was inspected by magnetic particle to ensure reliability. In this approach, the defects could be further excluded. The approach is an essential and simple measurement for component used in radiative region.

5.2 machining of the conical feature

In this part of the process, the machining tool requirements for the 4Cr13 stainless ball-pocket with hardness above HV600 are increased. Two machining methods of the conical feature were studied: turning with grinding wheel and milling with 5-axis machining, as shown in figure 10.

Given the error allowance of localization, the environmental temperature during machining should be the same as the operating temperature [15]. The influence of dimensional changes due to thermal expansions and contractions is an important factor [16]. The dimensional accuracy for 4Cr13 stainless ball-pocket directly determines the final performance of the locating structure and the aligning accuracy of the target equipment [17]. The coordinate measuring machine was used during the measuring of 4Cr13 stainless ball-pockets dimensions. The bearing ball was used as the benchmark for dimensioning [18]. The key dimensions include half cone angle, distance from the highest point of the bearing ball to the supporting face, and maximum radius of conical surface, as shown in figure 11. After the mean of many times measure was calculated, the maximum machining errors were 0.0139 degrees, 0.018 mm, and 0.0222 mm. These results indicate that the root mean square error in fit dimension chain was 0.02 mm [19]. It means that the machining error is less than the design accuracy of 0.2 mm. This root mean square error reflects the performance of one 4Cr13 stainless ball-pocket. The final aligning error is also related to the flatness error of the support, as well as the coaxial error between the ball-pocket and the base sheet [20]. Compared with the design accuracy, the final machining error of the 4Cr13 stainless ball-pocket should retain a definite allowance. It is useful for reasonable distribution of alignment allowance in practice, making equipment retainment considerably reliable [21].

6. Conclusions

(1) Derived from conical fit technology, 4Cr13 stainless ball-pocket was designed. This ball-pocket was also driven by the self-weight of the equipment being hoisted by overhead traveling crane. Moreover, 4Cr13 stainless ball-pocket is corelated with the bearing ball from coarse to fine, realizing ball-guided automatic aligning and easy dismantling in radiative region.

(2) Given the analysis result of stress distribution during alignment, 4Cr13 stainless steel was chosen to manufacture ball-pocket. After the three heat treatment parameters were investigated, it could successfully enhance the comprehensive mechanical properties of the 4Cr13 stainless ball-pocket, such as toughness, hardness and strength.

(3) The reasonable feed value and higher strength machining tool are crucial to ensure the machining error during the conical feature formation. The environmental temperature during machining should be same as the operating temperature.

(4) Given the advantages of the 4Cr13 stainless ball-pocket, such as automatic aligning and self-locking, this study could offer reliable strategy and measure for long-distance localization in radiative region as well as other dangerous regions.

Declarations

Acknowledgements

Not applicable

Funding

Supported by National Science Foundation of China (Grant No.12105308)

Availability of data and materials

The datasets supporting the conclusions of this article are included within the article.

Authors' contributions

The authors' contributions are as follows: Hua-Yan He was in charge of the whole trial and wrote the manuscript; Guang-Yuan Wang assisted with sampling and laboratory analyses.

Competing interests

The authors declare no competing financial interests.

Consent for publication

Not applicable

Ethics approval and consent to participate

Not applicable

References

[1] LI Lun. Radiation Dose Monitor System for CSNS[J]. Nuclear Electronics & Detection Technology, 2018, 38(6) :764-768.

[2] Y Jeong, D Lee, K Kim, et al. A wearable robotics arm with high force-reflection capability. Proceedings of the IEEE International Workshop on Robot and Human Interactive Communication, Osaka, Japan, September 27–29, 2000: 27–29.

[3] Wang Guofeng. Application of DB in the preassembling and pre-alignment of BEPCII[J]. URBAN GEOTECHNICAL INVESTIGATION & SURVEYING, 2008(1):112-115.

[4] Huang Zhencang. Inter-changeability and technology measurement[M]. Guangzhou: Southchina University of Technology Press, 2005:76-88.

[5] Nanyan Shen. A practical method of improving hole position accuracy in the robotic drilling process[J]. The International Journal of Advanced Manufacturing Technology, 2018 (9): 2973-2987.

[6] Yang zhen, Li Guangyun, He Liu. Measurement methods and precision analysis of optical collimation[J]. INFRARED AND LASER ENGINEERING, 2011,40(2):282-286.

[7] Ni jian, Tian Ruiqing. Positioning structure reliability technique of marine feed pump rotor pump impeller[J]. China Heavy Equipment, 2019(3):43-48.

[8] Shi Wen. Metal material and heat treatment[M]. Shanghai: Shanghai technology Press, 2011:14-26.

[9] Ma Jijun, Yang Shuai, Yu Jinming. Fatigue strength analysis of C groove structure of a-alloy train body under vibration load of suspension equipment[J]. Journal of Dalian Jiaotong University, 2015, 36(5) :26-29.

[10] Maciej Malicki. The impact of damage in anneling inconel 718 on hardness measured by tvickers method[J]. Fatigue of Aircraft Structures, 2016, 8:92-96.

[11] Zhu Qianhao, Ma Su. Heat treatment of large-sized AISI 4150H steel gear ring[J]. Heat Treatment, 2018, 33(6) :44-48.

[12] Shao Yujia, Yang Zhaojing, Wang Lingqi. Effect of hardening process on microstructure and hardness of high-nitrogen 40Cr15Mo2VN steel[J]. Heat Treatment, 2019, 34(2) :31-33, 36.

[13] Xue Shun, Tian Jun, Wang Wenhu, et al. Continuous cooling transformation curve and heat treatment process of a new type of spring steel used for high speed railway[J]. Hot Working Technology,

2013, 42(16) :176-179.

[14] A. Boudilmi, K. Loucif. Modelling of thin films Hardness measured by a spherical indenter[J]. METALLOFIZIKA I NOVEISHIE TEKHNOLOGII, 2018, 40(12) :1689-1697.

[15] da Silva Andrade Breno Henrique. Effects of annealing temperature on thermodynamic parameters and mechanical properties of a Cu-Al-Be-Nb-Ni-Cr alloy[J]. Materials letters, 2021, 302:1-4.

[16] Zixi Fang, Zezhong C Chen, et al. Simultaneous calibration of probe parameters and location errors of rotary axes on multi-axis machine tolls by inspecting a sphere[J]. Measurement, 2021, doi: https://doi.org/10.1016/j.measurement.2021.110389.

[17] Le Thi.Nhung. Effect of temperature on δ-Ferrite morphology of carbon steel and austenitic stainless steel welds [J]. Materials Science Forum, 2021, 6042(2068) :23-32.

[18] Hu Dongfang. The control of machining errors of tool path for unequal diameter flank milling of globoidal cam[J]. The International Journal of Advanced Manufacturing Technology, 2021, 113(9) :2999-3009.

[19] Ren Jie. In-beam g-rays of back-streaming white neutron source at China Spallation Neutron Source[J]. Acta Physica Sinica, 2020, 69(17) :233-241.

[20] Dongfang Hu. Tool path optimization algorithm of spatial cam flank milling based on NURBS surface[J]. Journal of the Brazilian Society of Mechanical and Engineering, 2018(40):1-8.

[21] Gao Jian, Chen Yueping, Deng Haixiang. In-situ inspection error compensation for machining accuracy improvement of complex components[J]. Journal of Mechanical Engineering, 2013, 49(9):133-143.

Figures

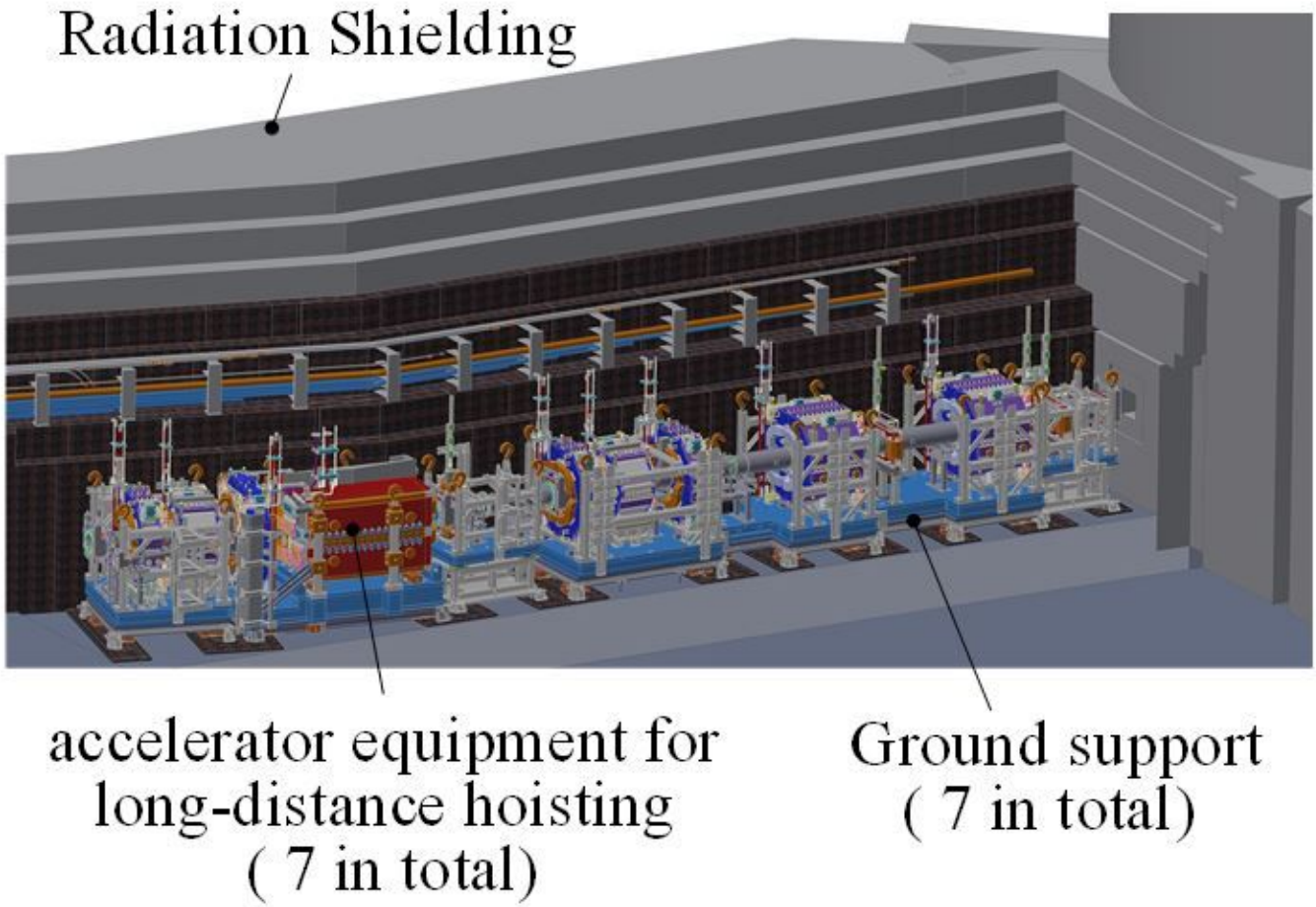

Figure 1

The equipment layout of proton transporting line nearby beam target

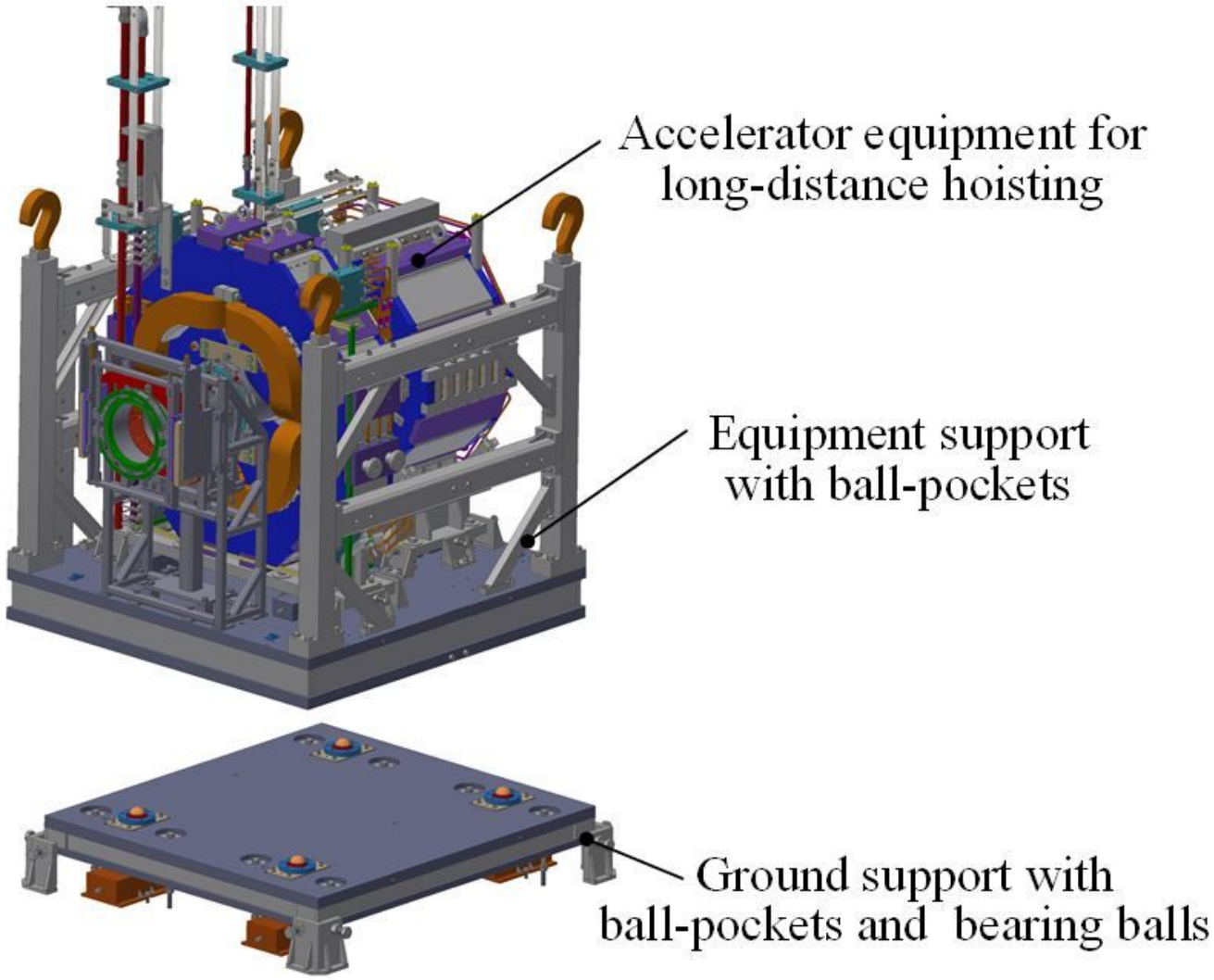

Figure 2

The sketch of equipment unit

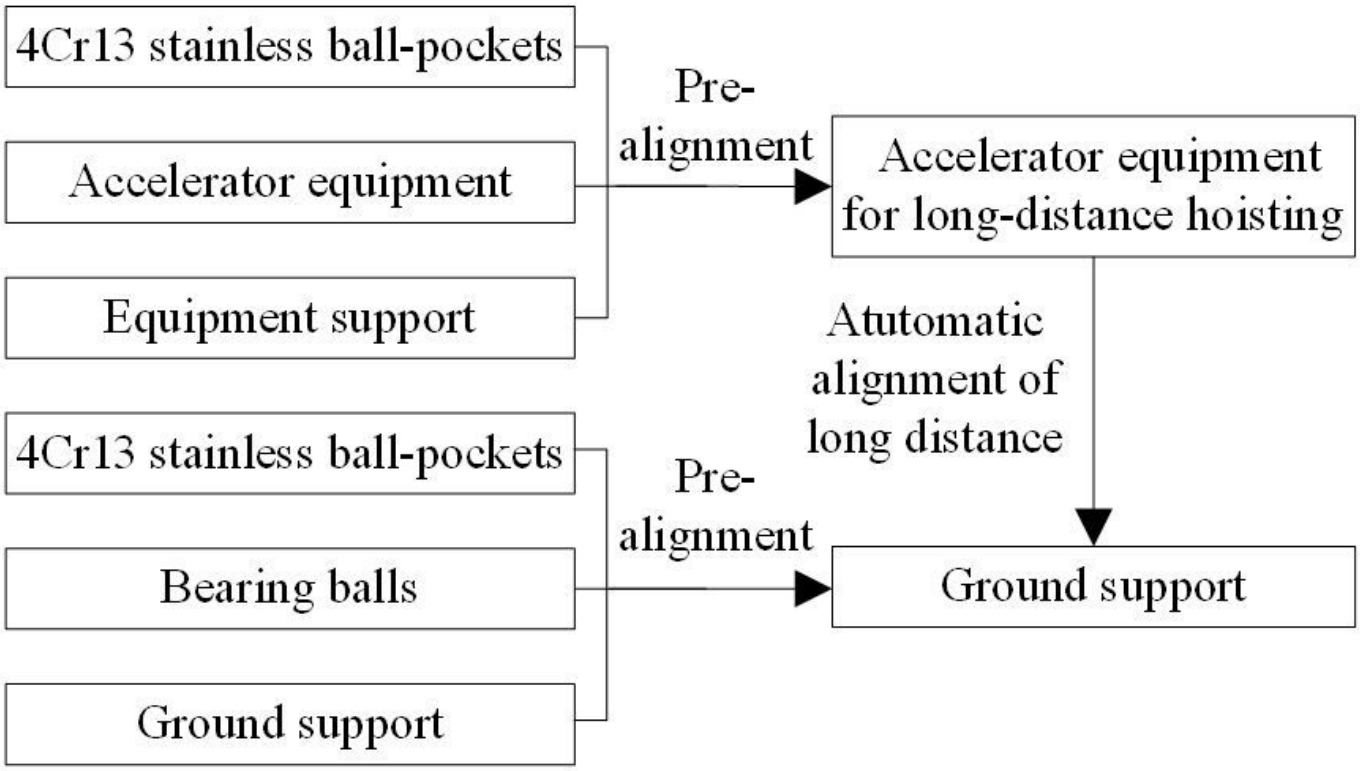

Figure 3

The flowchart of long-distance localization

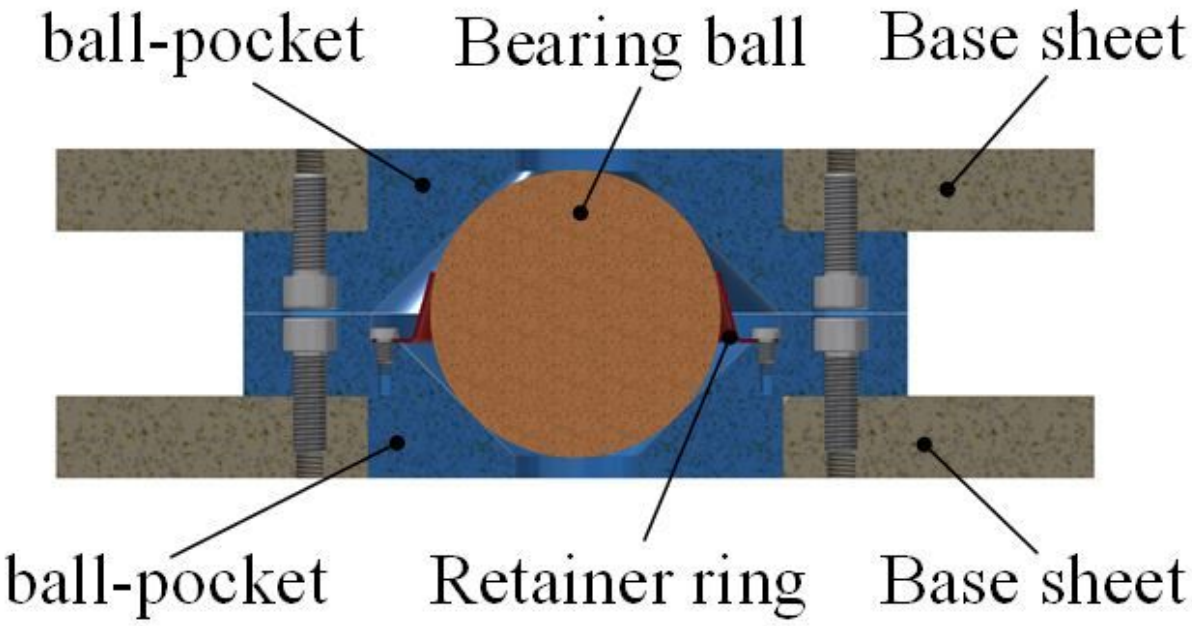

Figure 4

The sketch of locating structure

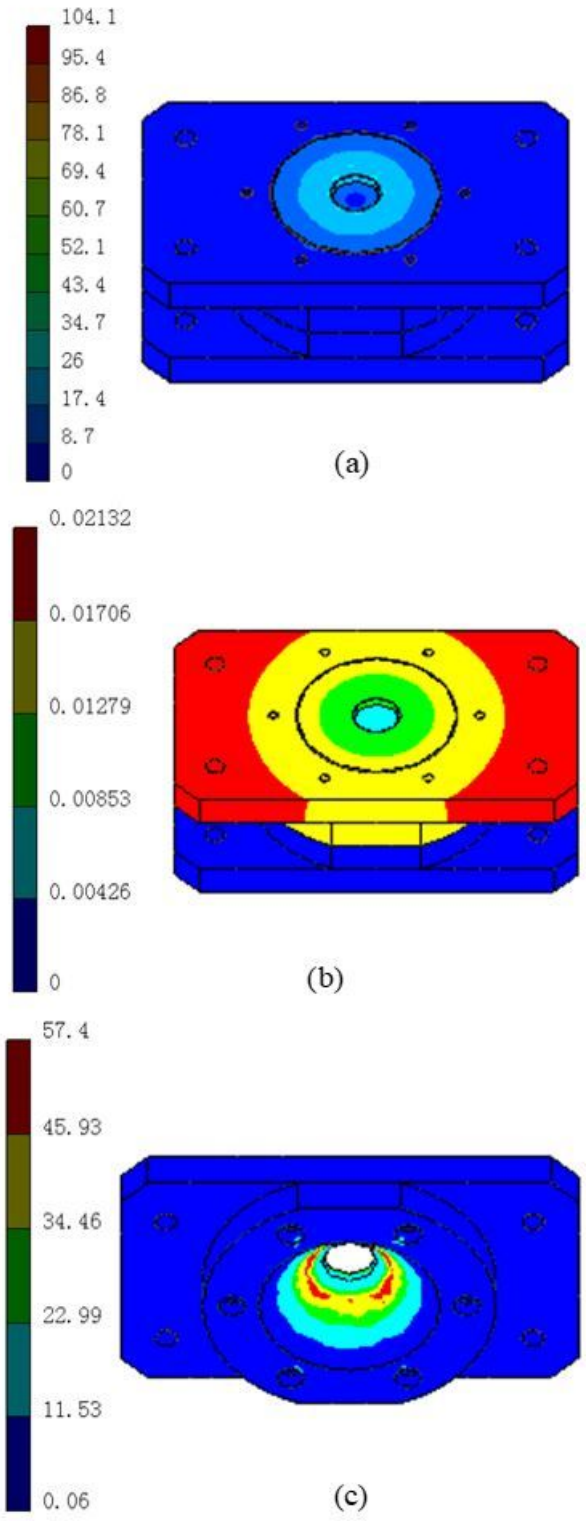

Figure 5

Equivalent stress distribution of the locating structure(a), deformation distribution of the locating structure(b) and Equivalent stress distribution of the 4Cr13 ball-pocket(c)

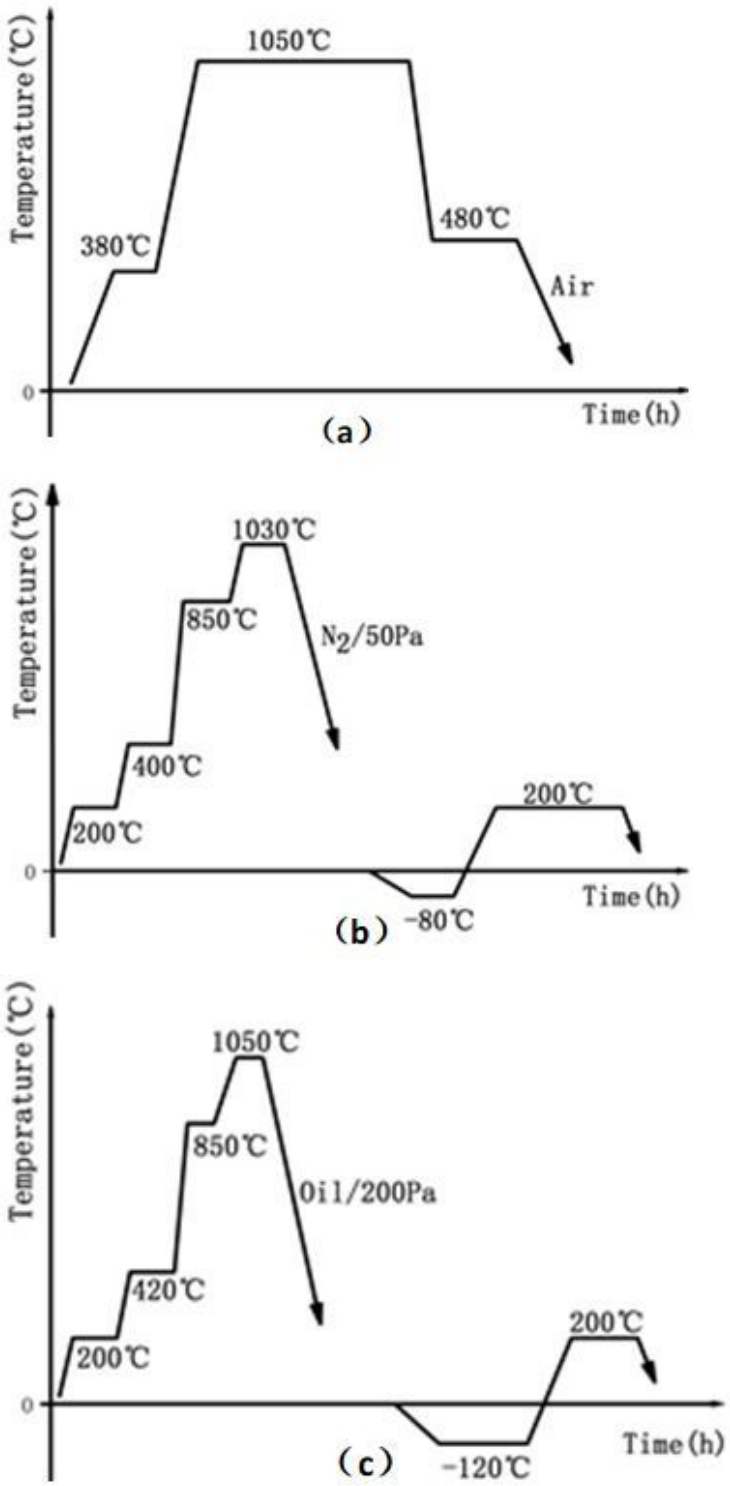

Figure 6

Three processes of heat treatment: empirical process a(a), optimized process b(b) and c(c) with cryogenic treatment and tempering

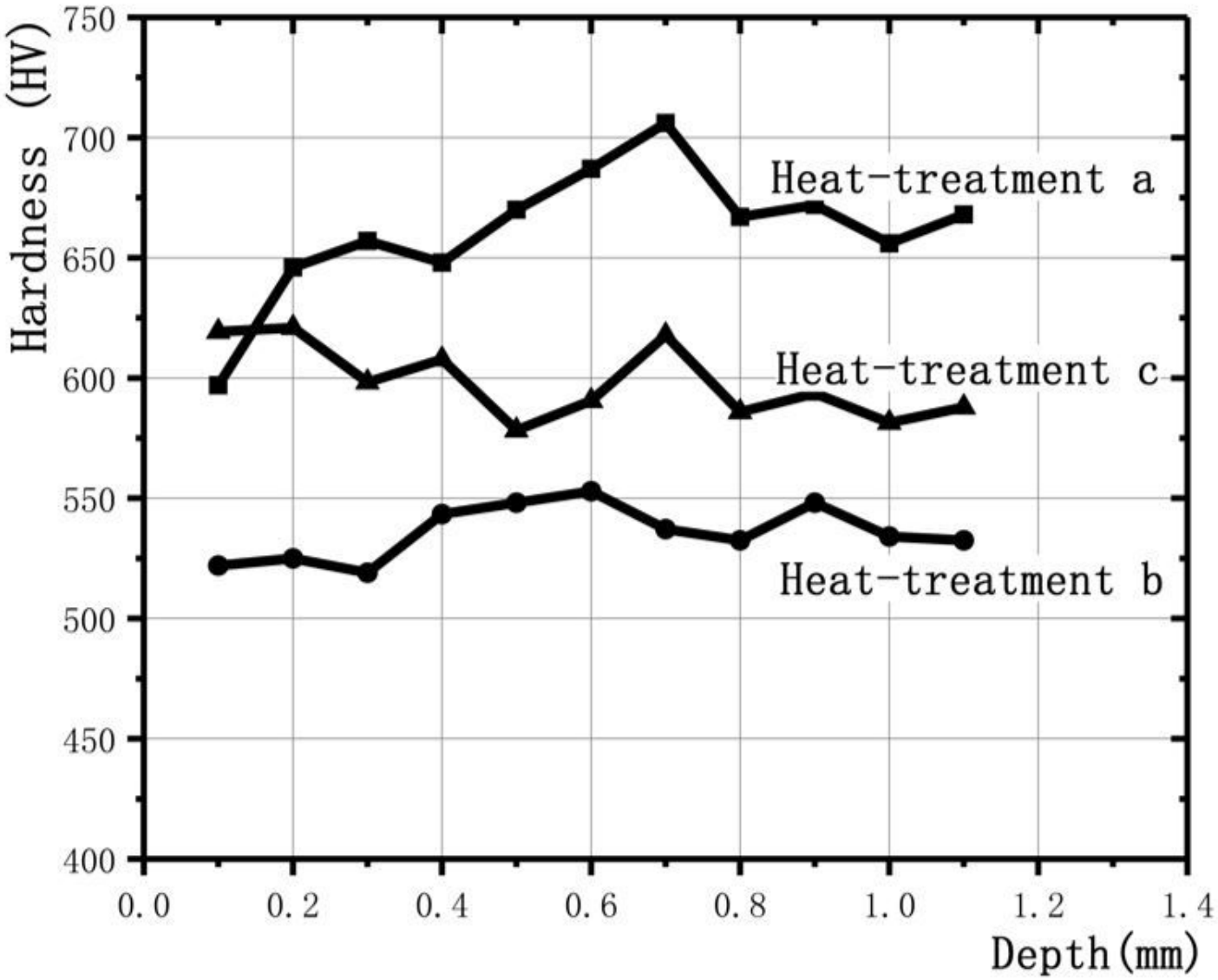

Figure 7

Measurement of hardness of 4Cr13 stainless ball-pocket

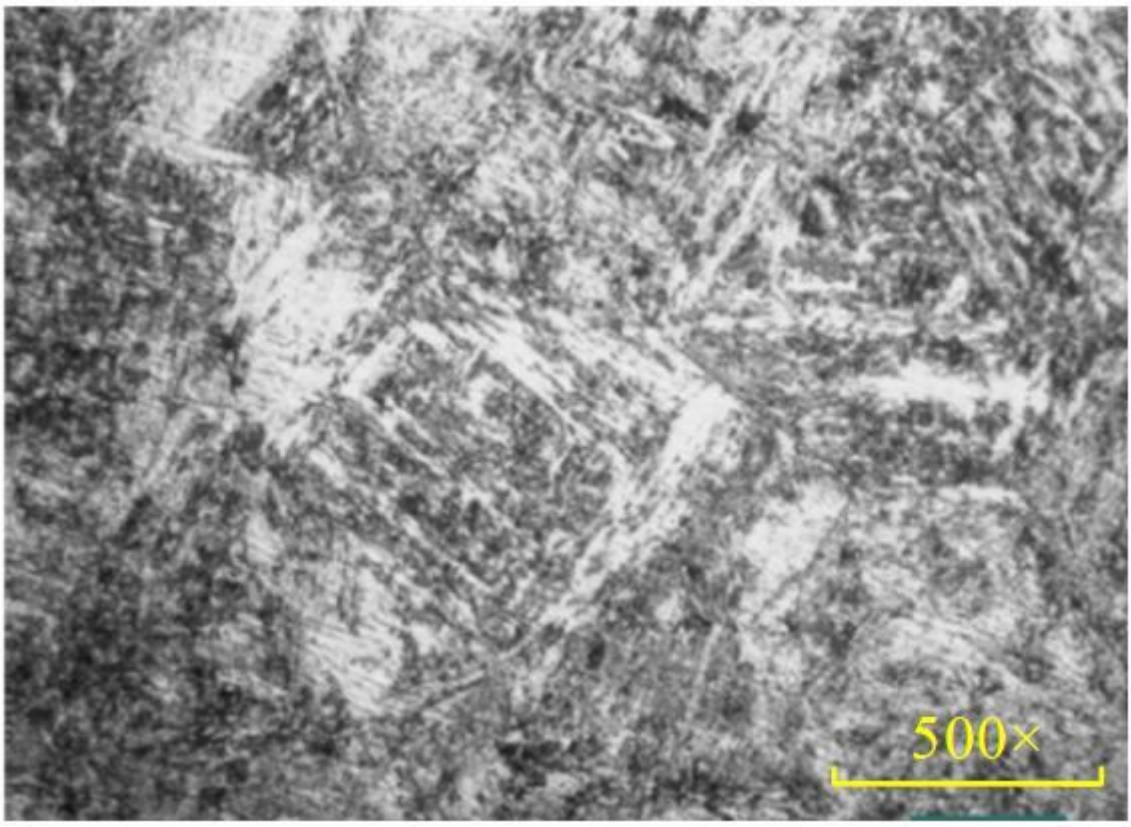

Figure 8

The cross-section image of microstructure for 4Cr13 stainless ball-pocket by process c of heat treatment

Figure 9

Inspection of magnetic particle for 4Cr13 stainless ball-pocket

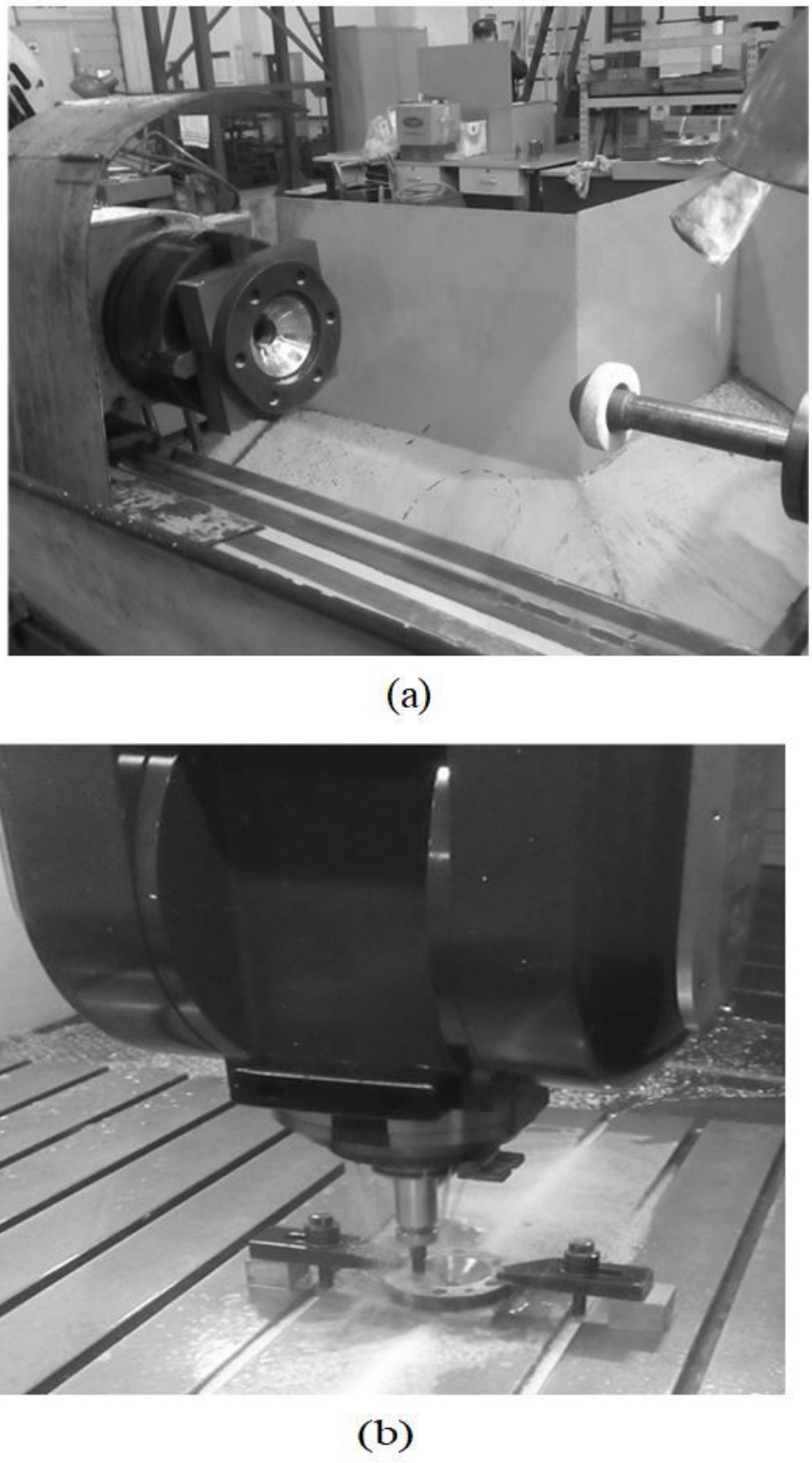

Figure 10

The method of forming conical feature: turning with grinding wheel (a) and milling with 5-axis machining (b)

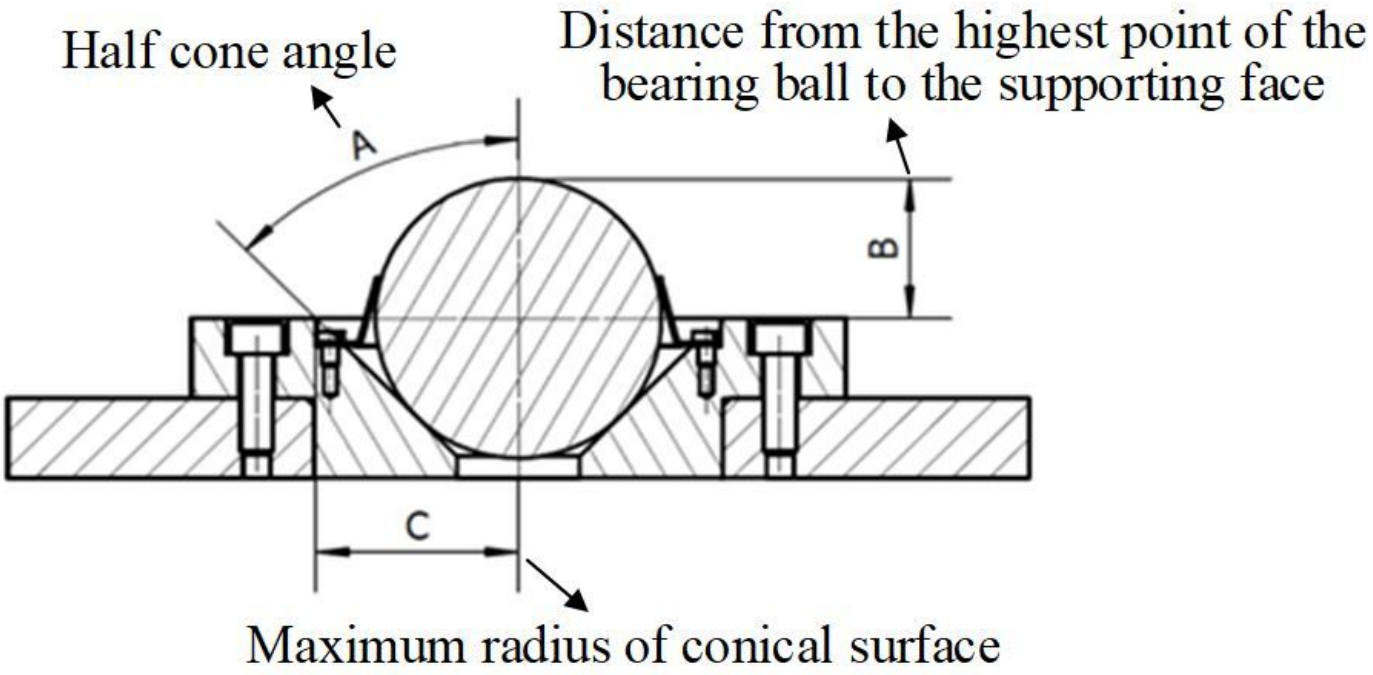

Figure 11

The check of key dimensions for 4Cr13 stainless ball-pocket.